5-1-2017

# Restriction Spectrum Imaging Improves Risk Stratification in Patients with Glioblastoma.

A P Krishnan

R Karunamuni

K M Leyden

T M Seibert

R L Delfanti

*See next page for additional authors*

HHS Public Access

Author manuscript

*AJNR Am J Neuroradiol*. Author manuscript; available in PMC 2017 November 01.

Published in final edited form as:

*AJNR Am J Neuroradiol*. 2017 May ; 38(5): 882–889. doi:10.3174/ajnr.A5099.

# Restriction Spectrum Imaging improves risk stratification in patients with glioblastoma

**AnithaPriya Krishnan, Ph.D.**[1], **Roshan Karunamuni, Ph.D.**[2], **Kelly M. Leyden, M.Res**[1], **Tyler M. Seibert, M.D., Ph.D.**[1,2], **Rachel L. Delfanti, M.D.**[3], **Joshua M. Kuperman, Ph.D.**[1,3], **Hauke Bartsch, Ph.D.**[1,3], **Pia Elbe, B.Sc**[1], **Ashwin Srikant, B.Sc**[1], **Anders M. Dale, Ph.D.**[1,3,4], **Santosh Kesari, M.D., Ph.D.**[6], **David E. Piccioni, M.D., Ph.D.**[4], **Jona A. Hattangadi-Gluth, M.D.**[2], **Nikdokht Farid, M.D.**[1,3], **Carrie R. McDonald, Ph.D.**[1,2,5,*], and **Nathan S. White, Ph.D.**[1,3,*]

[1]Multimodal Imaging Laboratory, University of California, San Diego, La Jolla, CA 92037

[2]Department of Radiation Medicine, University of California, San Diego, La Jolla, CA 92037

[3]Department of Radiology, University of California, San Diego, La Jolla, CA 92037

[4]Department of Neurosciences, University of California, San Diego, La Jolla, CA 92037

[5]Department of Psychiatry, University of California, San Diego, La Jolla, CA 92037

[6]Department of Translational Neuro-oncology and Neurotherapeutics, John Wayne Cancer Institute and Pacific Neuroscience Institute at Providence Saint John's Health Center, Santa Monica, CA

## Abstract

**Background—**ADC as a marker of tumor cellularity has been promising for evaluating response to therapy in patients with glioblastoma (GBM), but does not successfully stratify patients according to outcomes, especially in the up-front setting. Here we investigate if restriction spectrum imaging (RSI) an advanced diffusion imaging model, obtained after surgery but prior to radiation therapy (RT) could improve risk stratification in patients with newly-diagnosed GBM relative to ADC.

**Methods—**Pre-RT diffusion weighted and structural imaging of 40 patients with GBM were examined retrospectively. RSI and ADC based hyper-cellularity volume fractions (RSI-FLAIR$_{vf}$, RSI-CE$_{vf}$, ADC-FLAIR$_{vf}$, ADC-CE$_{vf}$) and intensities (RSI-FLAIR$_{90\%}$, RSI-CE$_{90\%}$, ADC-FLAIR$_{10\%}$, ADC-CE$_{10\%}$) within the contrast enhancement (CE) and FLAIR hyper-intensity (HI) VOIs were calculated. The association of diffusion imaging metrics, CE volume (CE$_{vol}$) and FLAIR-HI volume (FLAIR$_{vol}$) with progression-free survival (PFS) and overall survival (OS) were evaluated using Cox proportional hazard (CPH) models.

**Results—**Among the diffusion metrics, RSI-FLAIR$_{vf}$ was the strongest prognostic metric of PFS (p=0.036) and OS (p=0.007) in a multivariate CPH analysis, with higher values indicating earlier

Address for correspondence: N.S. White, Multimodal Imaging Laboratory, Suite C101; 8950 Villa La Jolla Drive, La Jolla, CA 92037; phone: 858-534-7102; fax: 858-534-1078; nswhite@ucsd.edu.

*contributed equally to this work as senior authors

progression and shorter survival. RSI-FLAIR$_{90\%}$ was also associated with OS (p=0.043) with higher intensities indicating shorter survival. None of the ADC metrics were associated with PFS/OS. CE$_{vol}$ exhibited a trend towards significance for OS (p=0.063).

**Conclusions—**RSI derived cellularity in FLAIR-HI regions may be a more robust prognostic marker than ADC and conventional imaging for early progression and poorer survival in GBM patients. However future studies with larger samples are needed to explore its predictive ability.

## Introduction

Glioblastoma (GBM) is the most common and aggressive malignant primary brain tumor. Unfortunately, there has been only incremental improvement in the 5-year survival rate in the past decade (1). The standard of care for newly-diagnosed GBM remains fairly uniform with maximal permissible surgical resection followed by radiotherapy (RT) with concurrent and adjuvant temozolomide (TMZ) (2). Currently, novel molecular and cellular targeted therapies for treating GBMs are being investigated with many of them now in phase II clinical trials (3). With the advent of these new therapies, and a recent study showing that radiation dose escalation to 75Gy (above the standard dose of 60Gy) is safe and possibly more effective in newly diagnosed GBM (4), stratification of patients at highest risk for early progression is imperative as more aggressive or experimental treatments may be pursued in these individuals. These treatment decisions are usually considered within the first several weeks post-surgery once any residual tumor has been identified, making the pre-RT imaging pivotal for guiding the course of treatment.

Conventional MRI, including T1-post contrast and FLAIR, are non-specific as the former represents the breakdown of the blood-barrier due to tumor and non-tumor related causes and the latter may represent tumor-related edema, post-radiation change, or any cause of gliosis. Advanced MRI techniques, such as DWI, may offer more specific information related to the underlying physiology of the tissue and may complement existing measures. ADC estimates the magnitude of water diffusion in relation to the physical barriers in its environment. It is frequently used as an imaging biomarker for tumor cellularity (5,6) and is inversely correlated with tumor cell density (7). However, it is important to note that at the typical b-values used clinically (b=0,1000 s/mm$^2$), the diffusion signal primarily arises from the extracellular space (8). Therefore, in addition to estimating cell density, the ADC calculated at these b-values is also influenced by factors such as edema and necrosis, subsequently making ADC a rather non-specific measure of tumor cellularity.

To account for the influence of edema and necrosis on ADC intensities in the tumor and peritumoral regions, histogram analysis of normalized ADC intensities (9,10) (nADC; normalized with respect to mean ADC in normal appearing white matter) and two Gaussian mixture modeling of the ADC intensities within the tumor (5,6) have been proposed. However, these statistical methods only seek to reclassify voxels within an ROI such that voxels with presumably solid tumor are included in the analysis while potentially problematic voxels that are confounded by partial voluming with edema and necrosis are removed. These methods have shown some promise for evaluating treatment response and predicting progression-free survival (PFS) in both the upfront (5,11) and recurrent (6,12)

setting following treatment with anti-angiogenic therapy. However, the utility of these ADC metrics for predicting response to standard chemoradiation has been less frequently explored. There is some data to suggest that although ADC intensities are not predictive of PFS or overall survival (OS) in the up-front setting (5,10), the volume of ADC with a large tumor burden (nADC<1.5; hyper-cellularity (HC) volume) within the T2 volume stratifies OS both pre (13) and post-surgery (9). But it is unclear if the hyper-cellularity (HC) volume was correlated with the underlying T2 volume and if its predictive value merely reflects the association of the T2 volume with survival. Multiple studies have used the increase or decrease of HC volume fraction (i.e., the HC volume defined with respect to the variation in a mixture of normal appearing white and gray matter) as a predictive marker for evaluating treatment response (14) since this metric may capture the percentage of the tumor that is highly cellular and is not correlated with the structural volumes. But the utility of HC volume fraction at individual time-points for early risk stratification has not been explored.

Multi-compartment models of diffusion based on advanced multi-shell acquisitions can provide a more straightforward approach for mitigating the confounding effects of edema and necrosis at the voxel level. In particular, restriction spectrum imaging (RSI) is an advanced diffusion imaging model that separates the relative contributions of hindered and restricted signals originating from extracellular and intracellular water compartments, respectively, using a multi-b-shell acquisition in conjunction with a linear mixture model (15–17). Furthermore, RSI incorporates geometrical information to disambiguate isotropic restricted diffusion in tumor cells from anisotropic restricted diffusion in elongated neuronal processes (axons/dendrites collectively called neurites). Previous studies have demonstrated the increased sensitivity and specificity of RSI over ADC and DWI in both brain tumors (18) and prostate cancer (19), and McDonald *et al.* have recently demonstrated that RSI cellularity is a stronger predictor of both PFS and OS in patients following treatment with bevacizumab relative to ADC (20). However, its utility for predicting survival in patients newly-diagnosed with GBM has not been explored.

Here we investigate the application of RSI for risk stratification in newly diagnosed, resected GBM. Our hypothesis is that RSI, due to its multi-b shell acquisition and its inherent ability to decouple diffusion signal within tumor cells from that of extracellular pathology (e.g., edema), would be a more robust marker of patient outcomes.

## Materials and methods

This institutional review board approved retrospective study included 45 patients with pathologically-confirmed primary GBM who had pre-RT MRIs (median 23 days; range 9–113 days from surgery and median 10 days; range 1–29 days before start of RT) that included standardized RSI and conventional imaging sequences acquired between January 2011 and Nov 2015. All patients were followed for at least 6 months (May 2016). Patient characteristics are shown in Table 1. PFS and OS were defined relative to the pre-RT scan. All scans were reviewed by a neuro-radiologist to ensure image quality and determine the basis for exclusion. Of the 45 eligible candidates: 17 patients underwent a second resection with histopathology confirming tumor in 14 and showing predominantly radiation necrosis in 3. Given the expected bias that would be introduced in the calculation of PFS and OS by

including patients with pathologically proven radiation necrosis, these 3 patients were excluded. The two patients who were excluded had a GTR with marked FLAIR hyper-intensity within the surgical cavity (presumed to be blood products or proteinaceous material) with associated high RSI and low ADC signal, which essentially masked any usable diffusion signal at the margins of the surgical cavity. Tumor progression was determined based on consensus between the treating neuro-oncologist and neuro-radiologist using the Response Assessment in Neuro Oncology (RANO) criteria (21). In the case of no progression or death, PFS was censored at the date of last stable imaging and OS was censored at the date of last contact.

### MRI acquisition and Image pre-processing

MRI was performed on a 3.0T GE Signa Excite HDx scanner equipped with an 8-channel head coil. The imaging protocol included pre- and post-Gadolinium 3D volumetric T1-weighted IR-SPGR sequences (TE/TR = 2.8/6.5ms; TI = 450ms; FA = 8°; FOV = 24cm; 0.93 × 0.93 × 1.2 mm) and a 3D T2-weighted FLAIR sequence (TE/TR = 126/6000ms; TI = 1863ms; FOV = 24cm; 0.93 × 0.93 × 1.2mm). For RSI, a single-shot pulsed-field gradient spin-echo (PGSE) EPI sequence was used (TE/TR = 96ms/17s; FOV = 24cm, matrix = 96×96×48, 2.5mm voxel size) with 4 *b*-values (*b* = 0, 500, 1500, and 4000 s/mm2), and 6, 6, and 15 unique diffusion directions for each non-zero b-value, respectively (~8 min scan time). Prior to analysis, raw data were corrected for geometric distortions due to susceptibility, gradient nonlinearities, and eddy currents (22). This was followed by correction of patient motion and rigid registration of the pre- and post-contrast 3D IR-SPGR images and the FLAIR images to each other using in-house software. The diffusion-maps were registered to the post-contrast images through the B0 images (b=0mm$^2$/s volume), which were registered to the FLAIR images.

ADC values were calculated from a tensor fit to the b = 0, 500 and 1500s/mm$^2$ data. Technical details of the RSI mathematical framework are described in their entirety elsewhere (15–17) and the model used has been applied in other recent publication (20). Briefly, the measured signal in each voxel was modeled as the sum of signals from four distinct tissue compartments: 1) the signal from water trapped within small spherical cells that is restricted in all directions, 2) the signal from water trapped in elongated neuronal processes (i.e. neurites) that is restricted in the transverse direction, 3) the signal from extracellular water that is hindered by cells and neuronal processes, and 4) the signal from free water residing in CSF-filled compartments. RSI “cellularity” estimates were computed by combining the signal fraction from the intracellular compartment [1] with the isotropic restricted component of the neurite compartment [2]. The RSI cellularity maps were finally transformed to a standard z-score by scaling each patient’s data by the population mean and standard deviation in normal appearing white matter of all patients in this study.

### VOIs

CE volumes ($CE_{vol}$) and FLAIR hyper-intensity (FLAIR-HI) volumes ($FLAIR_{vol}$) excluding the resection cavity and intrinsically T1 hyper-intense regions (i.e., post-surgical blood products) were segmented semi-automatically (Amira® software package, Visage Imaging, Inc.) on the co-registered post-contrast 3D IR-SPGR images and FLAIR images by a single

expert image analyst with 8 years of experience. For patients whose pre-RT scan was acquired within two weeks after surgery, the immediate post-surgery scan was used to exclude areas of restricted diffusion caused by resection-induced cytotoxic edema.

### Imaging metrics

In this study, we chose to evaluate the utility of both the HC intensities and HC volume fractions as prognostic factors of PFS and OS. Based on a recent study (19), the $90^{th}$ percentile of RSI cellularity values was selected for our analysis and the HC volume fraction was defined as the volume having an RSI cellularity Z score ≥ 1.5 within the CE and FLAIR-HI VOIs as the HC volume estimated with this pre-RT nADC threshold was successful in stratifying survival (9). Imaging metrics included in the analysis were the following: $FLAIR_{vol}$, $CE_{vol}$, the $90^{th}$ percentile of RSI cellularity values in the CE (RSI-$CE_{90\%}$) and in the FLAIR-HI (RSI-$FLAIR_{90\%}$) VOIs and the RSI based HC volume fraction in the CE (RSI-$CE_{vf}$) and FLAIR-HI (RSI-$FLAIR_{vf}$) VOIs. The following ADC metrics were estimated for comparing against the respective RSI metrics: the $10^{th}$ percentile of ADC (11) in the CE (ADC-$CE_{10\%}$) and in the FLAIR-HI (ADC-$FLAIR_{10\%}$) VOIs, and the ADC based HC volume fraction [ADC Z score ≤ 1.5] in the CE (ADC-$CE_{vf}$) and FLAIR-HI (ADC-$FLAIR_{vf}$) VOIs.

### Statistical Analysis

Univariate Cox Proportional Hazard (CPH) models were used to determine the contribution of resection type (STR – sub-total resection; GTR – gross total resection), age and gender to PFS and OS. Multivariate CPH models that included a single imaging metric combined with any significant clinical covariates were used to determine the relationship between each continuous pre-RT imaging metric and PFS/OS. Kaplan-Meier (KM) curves for the imaging metrics that were significant in the multivariate CPH models were obtained by dichotomizing the population based on their median value and were compared using a log-rank test. Due to the exploratory nature of the study, we did not control for type I error. P values < 0.05 were considered statistically significant (R3.2.2). Statistical analysis was performed using R version 3.2.2 (23)

## Results

### Clinical

Median PFS in the final cohort (N=40) was 8.4 months and median OS was 19.5 months. Nine patients progressed within 6 months, 24 patients progressed within 12 months, 30 patients progressed within 18 months and 33 patients progressed within 24 months. The results of univariate CPH analyses for the clinical and imaging metrics are summarized in Table 2. CPH models revealed that the resection type (STR-1 vs GTR-2) had a trend towards significance for PFS and was significant for OS (Table 2), hence it was included as a covariate in multivariate CPH analyses. Age and gender (male-1, female-2) were not predictive of PFS or OS in this cohort. Box plots of the imaging metrics are displayed in Figure 1 and the box plots split by the median PFS and OS excluding the values from the censored patients for the relevant metrics that achieved significance in Table 2 are displayed in supplementary Fig 1.

### CE and FLAIR-HI volumes

In a univariate CPH analysis, $CE_{vol}$ was significantly associated with PFS and OS (Table 2). When adjusted for resection type, $CE_{vol}$ was no longer significant for PFS and had a trend towards significance for OS (p=0.063; Table 3). The KM curves of the two groups obtained by a median split and compared using log-rank test were significantly different for PFS ($\chi^2(1)$ =4.7, p=0.029) but not for OS ($\chi^2(1)$ =3.1, p=0.078; Figure 2). Based on this stratification, the median PFS for the two groups was 218 and 338.5 days. $FLAIR_{vol}$ was not associated with PFS or OS.

### RSI and ADC metrics

In a multivariate CPH analysis, $RSI\text{-}FLAIR_{90\%}$ was significantly associated with OS (p=0.043) such that higher RSI intensities were associated with shorter survival (Table 3) and $RSI\text{-}FLAIR_{vf}$ was significantly associated with both PFS (p=0.036) and OS (p=0.007; Table 3) such that higher HC volume fractions were associated with earlier progression and shorter survival. None of the RSI metrics in the CE VOI were significant for PFS/OS.

The KM curves of the two groups obtained by a median split of $RSI\text{-}FLAIR_{vf}$ were significantly different for both PFS ($\chi^2(1)$ =6.1, p=0.013) and OS ($\chi^2(1)$ =7.7, p=0.005; Figure 2). The median PFS of the two groups was 201.5 and 367.5 days and the median OS of the two groups was 451 and 750.5 days. Despite a strong trend, stratification by the median $RSI\text{-}FLAIR_{90\%}$ did not yield significant group differences in PFS ($\chi^2(1)$ =2.8, p=0.095) and OS ($\chi^2(1)$ =3.4, p=0.065).

To understand the influence of the threshold for defining HC volume fraction on the prognostic value, we repeated the analysis with HC volume fraction defined with a threshold of RSI cellularity Z score ≥ 1 and ≥ 2. $RSI\text{-}FLAIR_{vf}$ at Z≥ 1 was significantly associated with PFS (p=0.03; HR=1.023) and OS (p=0.042; HR=1.027). While $RSI\text{-}FLAIR_{vf}$ at Z≥ 2 was significant for OS (p=0.009; HR=1.096), it was not significant for PFS (p=0.09; HR= 1.043). Similarly, we also explored the prognostic value of the absolute HC volume with Z≥1.5 and they were prognostic for OS ($HC_{vol}$ in CE: p=0.018, HR=1.543; FLAIR-HI: p=0.042, HR=1.262) in a multivariate CPH analysis. $HC_{vol}$ within CE was significant for PFS in a univariate analysis (p=0.025; HR=1.141) but was not significant in a multivariate analysis with resection type as a covariate.

In a univariate CPH analysis, none of the ADC metrics were associated with PFS (Table 2). The absolute ADC HC volumes with Z≤1.5 within the FLAIR-HI VOI was significantly prognostic of OS in a univariate CPH analysis (p=0.015; HR=58.89) but only had a trend towards significance (p=0.079; HR=20.06) after accounting for resection type in a multivariate CPH analysis and was not associated with PFS (univariate: p=0.138; HR=4.835). The ADC HC volumes within CE VOI were not associated with outcomes.

Representative images of two patients in this cohort with short (patient A) and long (patient B) PFS are shown in Figure 3. Patient A had lower $CE_{vol}$, $FLAIR_{vol}$ and $ADC\text{-}FLAIR_{10\%}$ but higher $RSI\text{-}FLAIR_{90\%}$, $RSI\text{-}FLAIR_{vf}$ and $ADC\text{-}FLAIR_{vf}$ than patient B, likely reflecting higher tumor cellularity in patient's FLAIR-HI region. RSI-cellularity maps exhibit greater

conspicuity in this region compared to ADC maps. Accordingly, patientA had shorter PFS and OS compared to patientB.

## Discussion

In the management of a highly aggressive tumor like GBM, the ability to stratify patient survival post-operatively is important as this information can directly impact therapeutic decision-making. In this study, we found RSI metrics to better stratify patients according to both PFS and OS compared to conventional imaging and ADC metrics. Unfortunately, $CE_{vol}$ and $FLAIR_{vol}$ may have limited prognostic value in this setting once the extent of the resection is considered. Glioblastoma patients often have a more infiltrative tumor pattern and possibly a more hypoxic tumor biology (24) with some of them responding poorly to radiotherapy or conventional chemotherapy (25). The non-specificity of these conventional metrics could potentially be due to the hypoxic tumors not having contrast enhancement and the presence of infiltrative tumors not having a noticeable signal in both T1 and T2 images. Hence, there is a need for better imaging metrics that perform reliably and may aid in identification of GBM patients at high risk for early recurrence and worse survival.

Among the imaging metrics, we found that the pre-RT RSI derived measures of cellularity within the FLAIR-HI region were associated with PFS and OS. The prognostic value of RSI appeared robust to the threshold used to determine the HC volume. Conversely, ADC metrics within the FLAIR-HI region were not associated with outcomes. Tumor progression results in areas of increased tumor cellularity (i.e., decrease in diffusivity) and also areas of increased edema (i.e., increase in diffusivity), both of which can occur simultaneously within an imaging voxel. Furthermore, post-surgery but pre-RT, a significant portion of the enhancing HC volume of the tumor has probably been resected and the residual HC tumor is interspersed with edema. As ADC is a composite measure, the effects of these two opposing factors may cancel each other out, therefore limiting the prognostic value of ADC. RSI overcomes this limitation by separating the diffusivities associated with intracellular, restricted diffusion from the extracellular effects of edema. In contrast to a previous study (9) the absolute ADC HC volume was not significantly associated with OS and this might be due to the inclusion of resection type as a covariate in the analysis. Even though the absolute RSI HC volume was prognostic of OS, the volume fraction was a stronger prognostic metric of PFS/OS. We did not find an association between any of our diffusion metrics in the CE region similar to that of previous studies (9,10). Although the reason for this is not clear, it is likely that the CE region was quite limited in size in most patients given the short interval between surgery and RT.

It is worth noting that other advanced imaging techniques, including perfusion (10), MR spectroscopic imaging (MRSI) (26) and PET (27) have also been shown to stratify outcomes in GBM patients. While perfusion imaging provides information on vascular density and flow, MRSI and PET provide metabolic information. Pre-RT perfusion imaging metrics have been shown to predict PFS (10) but perfusion is limited in the central core of a solid tumor with hypoxic cancer cells (28) and with anti-angiogenic therapy where the vasculature is normalized removing the leaky vessels in the tumor (29). Pre RT MRSI metrics are associated with both PFS and OS (26) but suffer from lower spatial resolution compared to

conventional, perfusion and diffusion MRI. Although diffusion metrics should perform better than perfusion and MRSI with hypoxic tumor and anti-angiogenic therapy, none of the previous studies have shown an association of pre-RT diffusion with outcomes. Here we show that RSI based cellularity is a prognostic metric of PFS and OS and may offer advantages over perfusion and MRSI in the pre-RT setting.

One of the main limitations of the current study is the small sample size obtained at a single institution. The current study represents our effort to explore the clinical utility of RSI in a highly controlled study where all the patients were scanned in the same scanner and all images were processed in a highly uniform manner that included robust corrections for motion and geometric distortions. Given our modest size, we might be underpowered to detect smaller associations between some of our imaging metrics and survival. The generalizability and reproducibility of our results will need to be tested in prospective, multi-site clinical trials across multiple vendor platforms. A second limitation is that the heterogeneity of the therapeutic approaches that each patient received following standard RT and TMZ made it difficult to stratify patients according to treatment regimen. However, our major finding is that RSI performed better than ADC and conventional imaging in the same patient cohort, which is not confounded by between patient treatment variance. Future studies with cohorts large enough to stratify patients according to the additional therapies received would be of great benefit for better delineating predictors of response to various therapies. Another possible limitation is that the tumors were segmented by a single imaging expert. Thus, intra and inter-observer variability of the tumor segmentations were not evaluated. In addition, although all patients had pathology confirmed GBMs at the outset, histological validation of tumor progression was not available for all patients. Furthermore, correlation with genomic information and molecular markers (such as MGMT and IDH status), which are known to provide prognostic information, could not be performed as these data were only available for a subset of the cohort (Table 1). Molecular information is now systematically collected for GBM patients at our institution facilitating future studies investigating the prognostic value of these markers. Although the results from our recent preclinical study [30] show that the RSI cellularity metric correlates with histopathological markers of cellularity, additional validation in GBM patients is warranted.

## Conclusion

Following surgery but prior to initiating RT, RSI derived cellularity in the FLAIR-HI region performs better than ADC and conventional imaging for risk stratification in GBM patients. Therefore, RSI could be potentially useful for identifying patients at highest risk for early progression and shorter survival. However, future studies with larger sample sizes are needed to explore its predictive ability.

## Supplementary Material

Refer to Web version on PubMed Central for supplementary material.

## Acknowledgments

Funding: National Science Foundation 1430082 and General Electric, Investigator Initiated Research Award BOK92325 (N.S.W); National Institute of Health R01NS065838 (C.R.M.), NIH RC2 DA29475 (A.M.D.) and EB00790-06 (A.M.D.); NIH UL1TR000100 (J.A.H.) and KL2TR00099 (J.A.H.); National Cancer Institute: Cancer Center Specialized Grant (P30CA023100; C.R.M.; J.A.H.); American Cancer Society Research Scholar Grant; RSG-15-229-01-CCE (C.R.M.) and ACS-IRG 70-002 (J.A.H.)

**Funding**

National Science Foundation Grant 1430082 (N.S.W.); General Electric, Investigator Initiated Research Award BOK92325 (N.S.W); National Institutes of Health grants R01NS065838 (C.R.M.); RC2 DA29475 (A.M.D.) and EB00790-06 (A.M.D.); National Cancer Institute Cancer Center Specialized Grant (P30CA023100; C.R.M.). National Institutes of Health UL1TR000100 (J.A.H.) and KL2TR00144 (J.A.H.); American Cancer Society Award ACS-IRG 70-002 (J.A.H.) and American Cancer Society RSG-15-229-01-CCE (C.R.M)

We would like to thank patients at the UCSD Moores Cancer Center Neuro-Oncology Program for their generous participation.

## Abbreviations

| | |
|---|---|
| **RSI** | Restriction Spectrum Imaging |
| **RANO** | Response Assessment in Neuro Oncology |
| **CPH** | Cox Proportional Hazard |
| **PFS** | Progression Free Survival |
| **OS** | Overall Survival |
| **STR** | sub-total resection |
| **GTR** | gross total resection |
| **RT** | Radiation Therapy |
| **KM** | Kaplan Meier |
| **CART** | Classification And Regression Tree |

## References

1. Ostrom QT, Gittleman H, Chen Y, et al. CBTRUS Statistical Report: Primary Brain and Central Nervous System Tumors Diagnosed in the United States in 2005–2009. Neuro Oncol. 2012; 14(suppl 5):1–21.
2. Stupp R, Mason WP, van den Bent MJ, et al. Radiotherapy plus Concomitant and Adjuvant Temozolomide for Glioblastoma. N Engl J Med. 2005 Mar 10; 352(10):987–96. [PubMed: 15758009]
3. Carlsson SK, Brothers SP, Wahlestedt C. Emerging treatment strategies for glioblastoma multiforme. EMBO Mol Med. 2014; 6(11):1359–70. [PubMed: 25312641]
4. Tsien CI, Brown D, Normolle D, et al. Concurrent Temozolomide and Dose-Escalated Intensity-Modulated Radiation Therapy in Newly Diagnosed Glioblastoma. Clin Cancer Res. 2012 Jan 1; 18( 1):273–9. [PubMed: 22065084]
5. Pope WB, Lai A, Mehta R, et al. Apparent Diffusion Coefficient Histogram Analysis Stratifies Progression-Free Survival in Newly Diagnosed Bevacizumab-Treated Glioblastoma. Am J Neuroradiol. 2011; 32(5):882–9. [PubMed: 21330401]

6. Ellingson BM, Sahebjam S, Kim HJ, et al. Pretreatment ADC histogram analysis is a predictive imaging biomarker for bevacizumab treatment but not chemotherapy in recurrent glioblastoma. AJNR Am J Neuroradiol. 2014; 35(4):673–9. [PubMed: 24136647]
7. Higano S, Yun X, Kumabe T, et al. Malignant astrocytic tumors: clinical importance of apparent diffusion coefficient in prediction of grade and prognosis. Radiology. 2006; 241(3):839–46. [PubMed: 17032910]
8. Mulkern RV, Gudbjartsson H, Westin C-F, et al. Multi-component apparent diffusion coefficients in human brain†. NMR Biomed. 1999 Feb 1; 12(1):51–62. [PubMed: 10195330]
9. Saraswathy S, Crawford F, Lamborn K, et al. Evaluation of MR markers that predict survival in patients with newly diagnosed GBM prior to adjuvant therapy. J Neurooncol. 2009; 91(1):69–81. [PubMed: 18810326]
10. Li Y, Lupo JM, Polley M-Y, et al. Serial analysis of imaging parameters in patients with newly diagnosed glioblastoma multiforme. Neuro Oncol. 2011; 13(5):546–57. [PubMed: 21297128]
11. Wen Q, Jalilian L, Lupo JM, et al. Comparison of ADC metrics and their association with outcome for patients with newly diagnosed glioblastoma being treated with radiation therapy, temozolomide, erlotinib and bevacizumab. J Neurooncol. 2015; 121(2):331–9. [PubMed: 25351579]
12. Pope WB, Kim HJ, Huo J, et al. Recurrent glioblastoma multiforme: ADC histogram analysis predicts response to bevacizumab treatment. Radiology. 2009; 252(1):182–9. [PubMed: 19561256]
13. Crawford FW, Khayal IS, McGue C, et al. Relationship of pre-surgery metabolic and physiological MR imaging parameters to survival for patients with untreated GBM. J Neurooncol. 2009; 91(3): 337–51. [PubMed: 19009235]
14. Ellingson BM, Cloughesy TF, Zaw T, et al. Functional diffusion maps (fDMs) evaluated before and after radiochemotherapy predict progression-free and overall survival in newly diagnosed glioblastoma. Neuro Oncol. 2012; 14(3):333–43. [PubMed: 22270220]
15. White NS, Leergaard TB, D'Arceuil H, et al. Probing tissue microstructure with restriction spectrum imaging: Histological and theoretical validation. Hum Brain Mapp. 2013 Feb 1; 34(2): 327–46. [PubMed: 23169482]
16. White NS, Dale AM. Optimal Diffusion MRI Acquisition for Fiber orientation Density Estimation: An Analytic Approach. Hum Brain Mapp. 2009 Nov; 30(11):3696–703. [PubMed: 19603409]
17. White NS, Dale AM. Distinct effects of nuclear volume fraction and cell diameter on high b-value diffusion MRI contrast in tumors. Magn Reson Med. 2014 Nov 1; 72(5):1435–43. [PubMed: 24357182]
18. White NS, McDonald CR, Farid N, et al. Improved Conspicuity and Delineation of High-Grade Primary and Metastatic Brain Tumors Using "Restriction Spectrum Imaging": Quantitative Comparison with High B-Value DWI and ADC. Am J Neuroradiol. 2013 May 1; 34( 5):958–64. [PubMed: 23139079]
19. McCammack, KC., Kane, CJ., Parsons, JK., et al. Prostate Cancer Prostatic Dis. Macmillan Publishers Limited; 2016. In vivo prostate cancer detection and grading using restriction spectrum imaging-MRI.
20. McDonald CR, Delfanti RL, Krishnan AP, et al. Restriction spectrum imaging predicts response to bevacizumab in patients with high-grade glioma. Neuro-Oncology. 2016 Apr 21.
21. Wen PY, Macdonald DR, Reardon DA, et al. Updated Response Assessment Criteria for High-Grade Gliomas: Response Assessment in Neuro-Oncology Working Group. J Clin Oncol. 2010 Apr 10; 28( 11):1963–72. [PubMed: 20231676]
22. Holland D, Kuperman JM, Dale AM. Efficient correction of inhomogeneous static magnetic field-induced distortion in Echo Planar Imaging. Neuroimage. 2010 Mar; 50(1):175–83. [PubMed: 19944768]
23. R Core Team. R: A language and environment for statistical computing. R Foundation for Statistical Computing; Vienna, Austria: 2013. URL http://www.r-project.org/
24. Vanan MI, Eisenstat DD. Management of high-grade gliomas in the pediatric patient: Past, present, and future. Neuro-Oncology Pract. 2014; 1(4):145–57.
25. Haar CP, Hebbar P, Iv GCW, et al. Drug Resistance in Glioblastoma: A Mini Review. Neurochem Res. 2015; 37(6):1192–200.

26. Li Y, Lupo JM, Parvataneni R, et al. Survival analysis in patients with newly diagnosed glioblastoma using pre- and post radiotherapy MR spectroscopic imaging. Neuro Oncol. 2013 May 1; 15( 5):607–17. [PubMed: 23393206]

27. Tralins KS, Douglas JG, Stelzer KJ, et al. Volumetric Analysis of 18F-FDG PET in Glioblastoma Multiforme: Prognostic Information and Possible Role in Definition of Target Volumes in Radiation Dose Escalation. J Nucl Med. 2002 Dec 1; 43( 12):1667–73. [PubMed: 12468518]

28. Eales KL, Hollinshead KER, Tennant DA. Hypoxia and metabolic adaptation of cancer cells. Oncogenesis. 2016 Jan 25.5(1):e190. [PubMed: 26807645]

29. Plate KH, Scholz A, Dumont DJ. Tumor angiogenesis and anti-angiogenic therapy in malignant gliomas revisited. Acta Neuropathol. 2012 Dec 11; 124(6):763–75. [PubMed: 23143192]

30. Hope TR, White NS, Kuperman J, et al. Demonstration of Non-Gaussian Restricted Diffusion in Tumor Cells Using Diffusion Time-Dependent Diffusion-Weighted Magnetic Resonance Imaging Contrast. Front Oncol. 2016 Aug 2.6:179. [PubMed: 27532028]

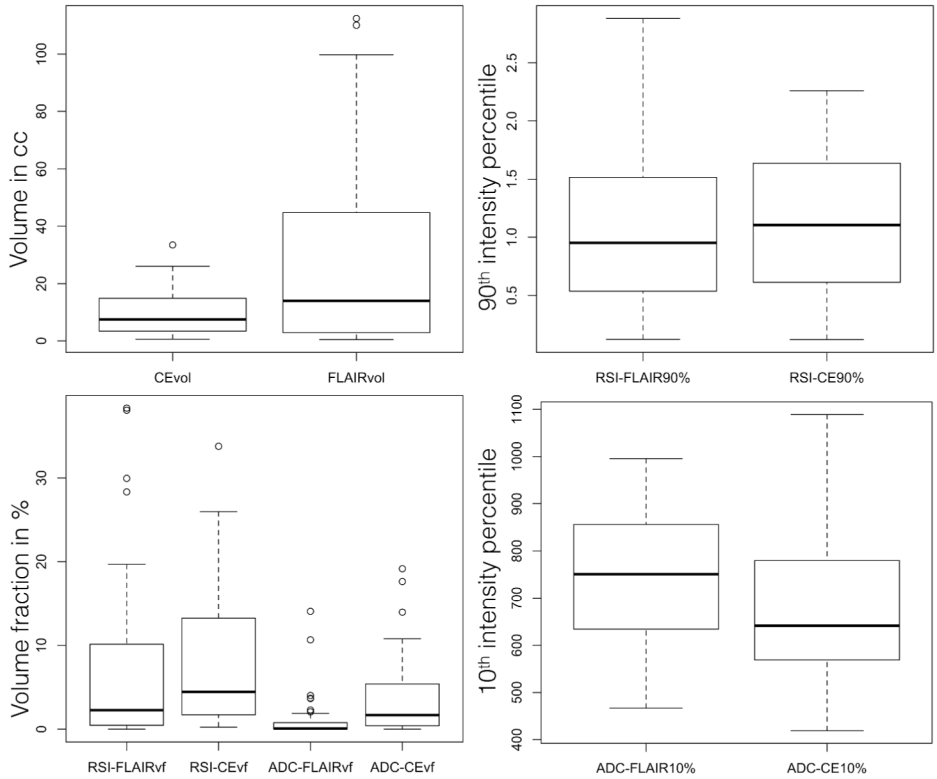


**Fig 1.**
Boxplots of the imaging metrics.

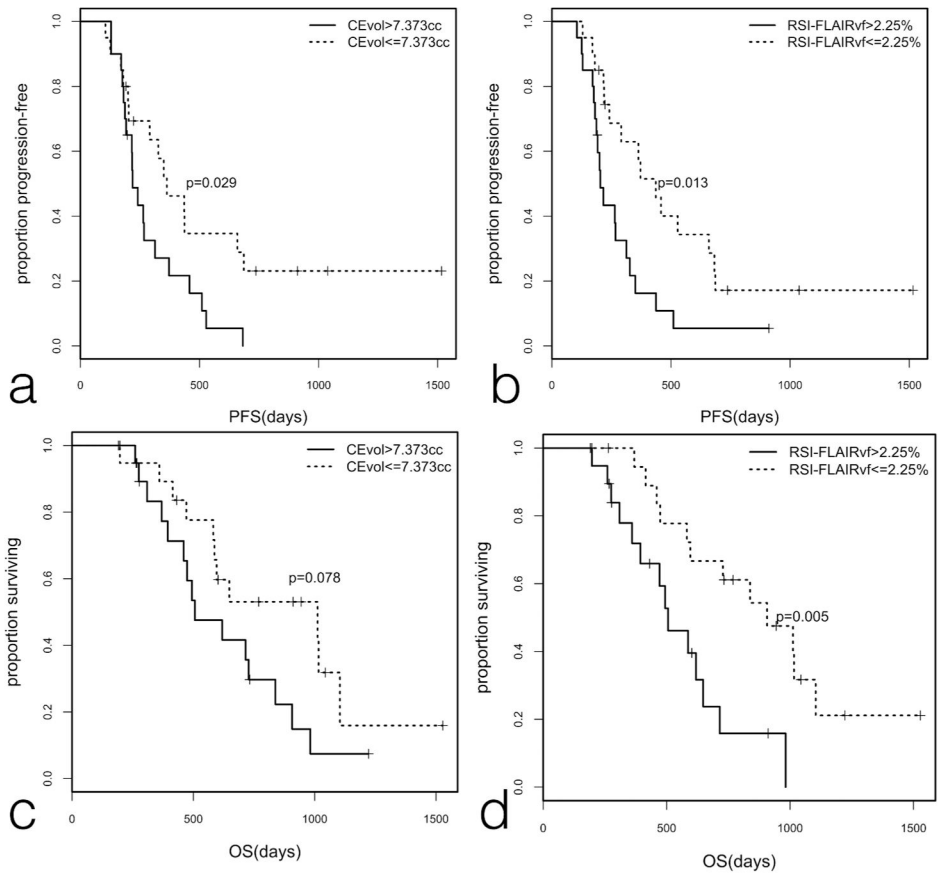


**Fig 2.**

Kaplan-Meier curves for the cohort stratified based on the median values for RSI-FLAIR$_{vf}$ for PFS [a] and OS [c]; and CE$_{vol}$ for PFS [b] and OS [d].

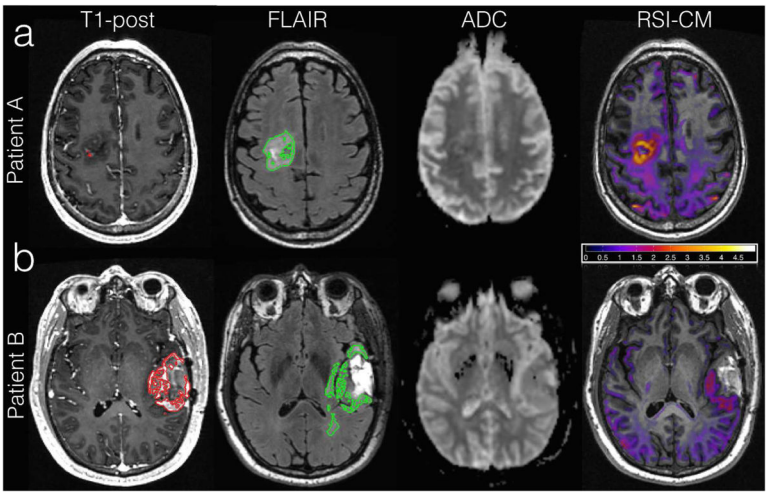


**Fig 3.**

Shown here are the axial T1 post, FLAIR, ADC and RSI-cellularity Z-score maps acquired post-surgery but pre-RT for two patients A and B. The VOI contours are shown in red and green for the CE and FLAIR-HI respectively. Patient A is a 63-year male with right posterior frontal GBM who underwent STR. This patient had high RSI cellularity in the FLAIR-HI region. Although there is corresponding ADC hypo-intensity in this region, it is subtle and inconspicuous. He had a shorter PFS and OS (PFS-4.2, OS-6.6 months) than Patient B. Patient B is a 31-year female with a right frontal GBM. There are no areas of high RSI cellularity or low ADC signal in the FLAIR-HI or CE region. He had a correspondingly longer PFS (PFS-14.5, OS-19.9 months).

**Table 1**

Patient characteristics

| | |
|---|---|
| Resection type[a] | STR (n=22); GTR (n=18) |
| Sex | 24 – male; 16 - female |
| Age: median [range] in yrs | 58 [31–84] |
| PFS: median [range] in months | 8.42 [3.5 – 50.53]; 7 censored |
| OS: median [range] in months | 19.48 [6.37–50.93]; 8 censored |
| Bevacizumab at recurrence | 17 patients |
| MGMT status | 12-unmethylated, 8-methylated, 20-unknown |
| IDH status | 15-WT[b], 25 - unknown |
| EGFR amplification | 7-unamplified, 12-amplified, 21-unknown |
| EGFRVIII status | 12-positive, 9-negative, 19-unknown |

[a]Resection type was determined from the immediate post-surgical scan acquired within 48 hours of surgery for all patients that included both T1-post contrast and FLAIR sequences.

[b]WT – wild type

**Table 2**

Results of univariate CPH analyses of the continuous clinical imaging metrics

| Metrics | PFS | | OS | |
|---|---|---|---|---|
| | **p value** | **HR [95% CI]** | **p value** | **HR [95% CI]** |
| Age | 0.562 | 0.992 [0.965 1.019] | 0.857 | 0.997 [0.965 1.03] |
| Gender | 0.063 | 0.512 [0.253 1.037] | 0.376 | 0.699 [0.316 1.546] |
| Resection type | 0.066 | 0.511 [0.249 1.046] | **0.002** | 0.235 [0.095 0.58] |
| $FLAIR_{vol}$ | 0.381 | 1.004 [0.994 1.014] | 0.404 | 1.005 [0.994 1.016] |
| $CE_{vol}$ | **0.047** | 1.04 [1.001 1.08] | **0.010** | 1.06 [1.014 1.108] |
| $ADC\text{-}FLAIR_{vf}$ | 0.397 | 0.939 [0.811 1.087] | 0.52 | 0.936 [0.766 1.145] |
| $ADC\text{-}CE_{vf}$ | 0.804 | 1.011 [0.925 1.105] | 0.932 | 0.995 [0.891 1.112] |
| $ADC\text{-}FLAIR_{10\%}$ | 0.384 | 1.001 [0.999 1.004] | 0.624 | 1.001 [0.998 1.004] |
| $ADC\text{-}CE_{10\%}$ | 0.735 | 0.999 [0.997 1.002] | 0.704 | 1.001 [0.998 1.003] |
| $RSI\text{-}FLAIR_{vf}$ | **0.038** | 1.031 [1.002 1.061] | **0.006** | 1.051 [1.015 1.089] |
| $RSI\text{-}CE_{vf}$ | 0.12 | 1.03 [0.992 1.069] | **0.021** | 1.048 [1.007 1.091] |
| $RSI\text{-}FLAIR_{90\%}$ | 0.092 | 1.522 [0.934 2.482] | **0.028** | 2.041 [1.081 3.855] |
| $RSI\text{-}CE_{90\%}$ | 0.154 | 1.507 [0.858 2.649] | 0.099 | 1.822 [0.893 3.716] |

## Table 3

Results of multivariate CPH analyses of the continuous imaging metrics co-varied with resection type

| Metrics | PFS | | OS | |
|---|---|---|---|---|
| | p value | HR [95% CI] | p value | HR [95% CI] |
| $RSI\text{-}FLAIR_{vf}$ | **0.036** | 1.033 [1.002 1.064] | **0.007** | 1.057 [1.015 1.100] |
| $RSI\text{-}CE_{vf}$ | 0.258 | 1.022 [0.984 1.062] | 0.183 | 1.028 [0.987 1.070] |
| $RSI\text{-}FLAIR_{90\%}$ | 0.097 | 1.535 [0.925 2.545] | **0.043** | 2.111 [1.024 4.350] |
| $RSI\text{-}CE_{90\%}$ | 0.210 | 1.439 [0.814 1.543] | 0.217 | 1.568 [0.767 3.203] |
| $FLAIR_{vol}$ | 0.845 | 1.001 [0.990 1.012] | 0.979 | 1.000 [0.989 1.011] |
| $CE_{vol}$ | 0.165 | 1.029 [0.988 1.073] | ***0.063*** | 1.044 [0.998 1.092] |